Journal of Chromatography B, 985 (2015) 91–102

Contents lists available at ScienceDirect

Journal of Chromatography B

journal homepage: www.elsevier.com/locate/chromb

Profiling and identification of the metabolites of baicalin and study on their tissue distribution in rats by ultra-high-performance liquid chromatography with linear ion trap-Orbitrap mass spectrometer

Jiayu Zhang[a,1], Wei Cai[b,1], Yuan Zhou[c], Ying Liu[a], Xiaodan Wu[d], Yun Li[b], Jianqiu Lu[a,*], Yanjiang Qiao[b,**]

[a] Center of Scientific Experiment, Beijing University of Chinese Medicine, Beijing 100029, China
[b] School of Chinese Pharmacy, Beijing University of Chinese Medicine, Beijing 100102, China
[c] The Institute of Vegetables and Flowers, Chinese Academy of Agricultural Sciences, Beijing 100081, China
[d] Department of Herbal Medicine, School of Basic Medical Sciences, Beijing University of Chinese Medicine, Beijing 100029, China

ARTICLE INFO

Article history:
Received 13 September 2014
Accepted 11 January 2015
Available online 23 January 2015

Keywords:
Baicalin
UPLC-ESI-MS/MS
Metabolic profile
Distribution
Multiple data processing method

ABSTRACT

Baicalin (baicalein 7-*O*-glucuronide), which is one of the major bioactive constituents isolated from Scutellariae Radix, possesses many biological activities, such as antiallergic, antioxidation, and anti-inflammatory activities. In the present study, an efficient strategy was established using ultra-high-performance liquid chromatography coupled with linear ion trap-Orbitrap mass spectrometer (UPLC-LTQ-Orbitrap MS) to profile the *in vivo* metabolic fate of baicalin in rat plasma, urine, and various tissues. A combination of post-acquisition mining methods including extracted ion chromatogram (EIC) and multiple mass defect filters (MMDF) was adopted to identify the common and uncommon baicalin metabolites from the full mass scan data sets. Their structures were elucidated based on the accurate mass measurement, relevant drug biotransformation knowledge, the characteristic collision induced fragmentation pattern of baicalin metabolites, and bibliography data. Based on the proposed strategy, a total of 32 metabolites were observed and characterized. The corresponding reactions *in vivo* such as methylation, hydrolysis, hydroxylation, methoxylation, glucuronide conjugation, sulfate conjugation, and their composite reactions, were all discovered in the study. The results demonstrated that the rat liver and kidney are the most important organs for the baicalin metabolites presence. Six metabolites might play an important role in exerting pharmacological effects of baicalin *in vivo*. The newly discovered baicalin metabolites significantly expanded our understanding on its pharmacological effects, and could be targets for future studies on the important chemical constituents from herbal medicines.

1. Introduction

Scutellariae Radix (the root of *Scutellariae baicalensis* Georgi) has been widely used as an important medicinal herb in China and other East Asian countries for treatment of various ailments including fevers, ulcers, cancers, and inflammation [1–3]. Baicalin (baicalein 7-*O*-glucuronide) (shown in Fig. 1), which is one of the major bioactive constituents isolated from Scutellariae Radix, possesses many biological activities, such as antiallergic, antioxidation and anti-inflammatory activities [4]. With the increasing attention on baicalin, it is important to extensively study the information regarding absorption, distribution, metabolism, and excretion (ADME), among which the characterization of metabolites can help to explain and predict a variety of events related to the efficacy and toxicity of baicalin [5,6]. However, to our best knowledge, the biotransformation of baicalin has been poorly understood, although some works on the metabolism of baicalin have already been performed [7–10]. For example, only 9 metabolites were isolated and identified from urine and feces of Wistar rats, which is due in part to the difficulties in obtaining enough amounts for NMR detection to identify more trace metabolites [8].

Abbreviations: ADME, absorption, distribution, metabolism and excretion; HRMS, high-resolution mass spectrometry; UPLC-LTQ-Orbitrap, ultra-high-performance liquid chromatography coupled with a linear ion trap-Orbitrap mass spectrometer; SD, Sprague-Dawley; EIC, extracted ion chromatogram; MDF, mass defect filtering; MMDF, multiple mass defect filtering; NLF, neutral loss filtering; IPF, isotope pattern filtering; CMC-Na, carboxymethyl cellulose sodium; RDB, ring and double bond; CID, collision induced dissociation; CE, collision energy; TIC, total ion chromatogram.

* Corresponding author. Tel.: +86 01064286203.
** Corresponding author. Tel.: +86 01084738621.
E-mail addresses: lujq@vip.sina.com (J. Lu), yanjiangqiao@sina.com (Y. Qiao).
[1] The first two authors contributed equally to this work.

http://dx.doi.org/10.1016/j.jchromb.2015.01.018
1570-0232/

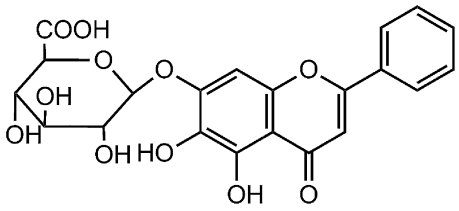

Fig. 1. Structure information of baicalin.

Recently, with the development of various data acquisition methods, liquid chromatography–mass spectrometry, especially for high-resolution mass spectrometry (HRMS), has exhibited excellent performances in metabolites detection owing to its high-speed and high detection sensitivity [11]. For example, linear ion trap-Orbitrap mass spectrometer (LTQ-Orbitrap) used in the present study has combined high trapping capacity and MS^n scanning function of the linear ion trap along with accurate mass measurements within 5 ppm and a resolving power of up to 100,000. Particularly, the Orbitrap facilitates fast data-dependent acquisition of accurate MS^n spectra on an LC timescale, which could increase the throughput and identification efficiency of metabolites. Moreover, a number of off-line LC–MS data mining methods are developed to identify the trace metabolites overwhelmed by interferences from the background or the matrix. For example, multiple data processing technologies including extracted ion chromatogram (EIC), mass defect filter (MDF), multiple mass defect filters (MMDF), product ion filtering (PIF), neutral loss filtering (NLF), and isotope pattern filtering (IPF) have been successfully applied to the identification of complex compounds or metabolites [12–15].

Herein, the comprehensive profiling and identification of *in vivo* metabolism of baicalin in plasma and urine of Sprague-Dawley rats was performed. A metabolism identification strategy based on the integration of ultra-high-performance liquid chromatography (UPLC)-LTQ-Orbitrap mass spectrometer with multiple data processing techniques was developed for characterizing the major-to-trace metabolites of baicalin in the rat plasma and urine. At the same time, the established method was further applied to elucidate the distribution of baicalin metabolites in various rat tissues.

2. Experimental

2.1. Chemicals and materials

Authentic standards, *viz.*, baicalin, baicalein, scutellarin, wogonoside, and oroxin A, were purchased from Chengdu Biopurify Phytochemicals Ltd. (Chengdu, China). Their structures were fully elucidated by the comparison of their spectra data (ESI-MS and ^1H, ^{13}C NMR) with those published literature values. The purities were higher than 98% according to HPLC/UV analysis.

HPLC grade acetonitrile and methanol were purchased from Fisher Scientific (Fair Lawn, NJ, USA). Formic acid (99%) was purchased from Sigma–Aldrich (St. Louis, MO, USA). Grace Pure™ SPE C18-Low solid-phase extraction cartridges (200 mg/3 mL, 59 μm, 70 Å) were purchased from Grace Davison Discovery Science™ (Deerfield, IL, USA). All the other chemicals of analytical grade from Beijing Chemical Works (Beijing, China) are commercially available. Deionized water used throughout the experiment was purified by a Milli-Q Gradient A 10 System (Millipore, Billerica, MA, USA). The 0.22 μm membranes were purchased from Xinjinghua Co. (Shanghai, China).

2.2. Animals

Eight male Sprague-Dawley (SD) rats (220–240 g) were purchased from Beijing Weitong Lihua Biotechnology Co., Ltd. (Beijing, China). The animals were housed individually under a constant temperature of 22 ± 1 °C and humidity of 50 ± 10%. The rats were randomly divided into two groups: Group A (n = 4), drug group for plasma, urine, and tissues; Group B (n = 4), control group for blank plasma, urine, and tissues. They were fasted for 12 h with free access to water prior to experiments. The animal protocols were approved by the institutional Animal Care and Use Committee at Beijing University of Chinese Medicine. The animal facilities and protocols were strictly consistent with the Guide for the Care and Use of Laboratory Animals (U.S. National Research Council, 1996).

2.3. Drug administration and biological samples preparation

Baicalin was suspended in 0.5% carboxymethylcellulose sodium (CMC-Na) aqueous solution and orally administered to rats of Group A at a dose of 400 mg/kg body weight. A 2 mL aliquot of 0.5% CMC-Na aqueous solution was administrated to each rat in Group B. 0.8 mL blood samples were withdrawn from the suborbital venous plexus of rats at 0.5, 1, 2, and 4 h post-dosing. Each sample was transferred to a heparinized micro-centrifuge tube and centrifuged at 14,000 rpm for 10 min to obtain plasma. The organs including heart, liver, spleen, lung, kidney, and brain, were respectively removed from two rats in Group A and Group B at 4 h post-dosing and washed with cold biological saline. Homogenates of heart, liver, spleen, lungs, kidneys, and brain were prepared by a homogenizer (DY89-11, Ningbo Scientz Biotechnology Co., Ltd., Ningbo, China) at 1000 rpm for 3 min at 4 °C, which were suspended in biological saline at a ratio of 1.0 g of tissue to 5 mL of biological saline. Then the homogenates were centrifuged at 5000 rpm for 15 min at 4 °C. The supernatant was separated out and processed using the below described method. Urine samples were collected over 0–24 h after the oral administrations (two rats in each group were sacrificed at 4 h). Finally, all biological samples from the same group were merged into one sample.

All the biological samples were prepared by a solid-phase extraction (SPE) method. An SPE cartridge was pretreated with 5 mL of water, 5 mL of methanol and 5 mL of water, successively. 1 mL sample of plasma or urine or the tissue solution was vortexed, loaded, and allowed to flow through the SPE cartridge with gravity, respectively. The SPE cartridge was washed with 5 mL of water and 3 mL of methanol, successively. The methanol eluate was collected and evaporated to dryness under N_2 at room temperature. The residue was re-dissolved in 100 μL of acetonitrile/water (10:90, v/v) and centrifuged at 14,000 rpm for 10 min. A volume of 5 μL supernatant was injected into UPLC-ESI-LTQ-Orbitrap MS for analysis.

2.4. UPLC analysis

An Accela 600 pump LC system (Thermo Scientific, Bremen, Germany) was used equipped with a binary pump and an autosampler. A Waters ACQUITY BEH C_{18} column (2.1 × 100 mm i.d., 1.7 μm) was used for separation of the metabolites at room temperature. Acetonitrile/methanol 3:1 (solvent B) and 0.5% formic acid aqueous solution (solvent A) were used as mobile phase. The flow rate was 0.3 mL/min applied with a linear gradient as follows: 0–15 min, 10–45% B; 15–18 min, 45–68% B; 18–20 min, 68–70% B; 20–21 min, 70–10% B; 21–24 min, 10% B.

2.5. LTQ-Orbitrap MS^n analysis

High-resolution ESI-MS and MS/MS spectral analysis were performed on an LTQ-Orbitrap mass spectrometer (Thermo Scientific, Bremen, Germany) connected to the HPLC instrument *via* ESI interface. Samples were analyzed in the negative ion mode with the tune method set as follows: sheath gas (nitrogen) flow rate of 30 arb, aux gas (nitrogen) flow rate of 5 arb, spray voltage of 4.0 kV, capillary temperature of 350 °C, capillary voltage of 25 V, tube lens voltage of 110 V. Accurate mass analysis was calibrated according to the manufacturer's guidelines using a standard solution mixture of caffeine, sodium dodecyl sulfate, sodium taurocholate, the tetrapeptide MRFA (Met-Arg-Phe-Ala) acetate salt and Ultramark. The measured masses were within 5 ppm of the theoretical masses. Centroided mass spectra were acquired in the mass range of m/z 100–800.

In the full scan experiment, resolution of the Orbitrap mass analyzer was set at 30,000 (full width at half maximum as defined at m/z 400). Data-dependent MS/MS scanning was performed to minimize total analytical time as it can trigger fragmentation spectra of target ions. The collision energy for collision induced dissociation (CID) was adjusted to 30% of maximum, and the isolation width of precursor ions was m/z 2.0 Da. The dynamic exclusion to prevent repetition was enabled, and the repeat count was set at 5 with the dynamic repeat time at 30 s and dynamic exclusion duration at 60 s.

2.6. Peak selections and data processing

Thermo Xcaliber 2.1 workstation was used for the data acquisition and processing. In order to obtain as many fragment ions of the metabolites as possible, the peaks detected with intensity over 30,000 were selected for identification. The chemical formulas for all parent ions of the selected peaks were calculated from the accurate mass using a formula predictor by setting the parameters as follows: C [0–30], H [0–50], O [0–20], S [0–4], N [0–4], Cl [0–4], and ring double bond (RDB) equivalent value [0–15]. Other elements such as P and Br were not considered because they are rarely present in the complex matrix.

3. Results and discussion

A total of 32 metabolites of baicalin were detected in the rat plasma and urine using UPLC-LTQ-Orbitrap mass spectrometer in combination with multiple data mining methods including the EIC and MMDF post data-mining methods. The detected metabolites were listed in Table 1.

3.1. Optimum conditions for UPLC-ESI-LTQ-Orbitrap analysis

The substances under investigation are flavonoid metabolites with some hydroxy groups, which make it predestined by ESI in negative ion mode. MS conditions were optimized on a UPLC-LTQ-Orbitrap MS instrument using the standard solution of baicalin (5 μg/mL). To achieve the optimized collision energy that generates adequate fragment information for structural elucidation and characterization, a series of ESI-MS/MS experiments were carried out at different collision energy (CE, 10–100%). By gradually increasing the CE, the intensity of product ions was first increased to maximum and then gradually decreased. Even though the optimum CE might vary for different metabolites, the result demonstrated that 30% CE was sufficient to yield abundant fragment ions for the structural elucidation.

3.2. Analytical strategy

A novel strategy was proposed for the systematic screening and characterization of baicalin metabolites on the HRMS instrument with data acquisition and multiple post-acquisition data processing techniques. First, the full mass scan was performed and MS/MS data sets were obtained using data-dependent acquisition method. Second, for the subsequent post-acquisition mining processing, using Thermo Networks software (Thermo Scientific, Bremen, Germany), a combination of EIC and MMDF methods was adopted to identify the baicalin metabolites. The molecular weights and the elemental compositions of common and uncommon metabolites derived from the accurate mass measurements can be rapidly predicted. Finally, the structures of metabolites were elucidated based on the accurate mass measurement, relevant drug biotransformation knowledge, the characteristic fragmentation pathways of baicalin metabolites, and bibliography data. The general procedures of our strategy and approach are summarized into a diagram as shown in Fig. 2.

3.3. Establishment of post-acquisition processing methods

In order to reduce the potential interferences of endogenous substance, the post-acquisition processing method of high-resolution EIC and MMDF was developed for metabolite detection including low levels of predicted and unpredicted metabolites. Generally speaking, the high-resolution EIC process with m/z values calculated is highly effective in the detection of common compounds with predictive molecular weights. Therefore, high-resolution EICs of baicalin metabolites were detected by processing the full-scan MS data sets using predictive metabolite weights within 5 ppm mass tolerance. Meanwhile, based on the similarity of mass defects of metabolites and their core substructures, the MMDF method can be adopted to search for the relevant compounds, especially the uncommon compounds that could not be detected by the EIC method [16]. Therefore, the combination of full-scan MS-based EIC and MMDF methods can be adopted to target both common and uncommon metabolites.

For MMDF method, the first and most important step was to set the metabolite templates. The frequently used MDF templates are: drug filter, substructure filter, and conjugate filter. Since baicalin is difficult to yield two smaller molecules through the cracking reaction, five templates (drug filter, substructure filter, and three conjugate filters) were used in parallel to screen the metabolites. The second step was to confirm the mass defect range according to the templates mentioned above. Each MDF window was set to ±50 mDa around the mass defects of the templates over a mass range of ±50 Da around the filter template masses. Finally, the parent drug filter template was based on the location of baicalin ($C_{21}H_{17}O_{11}$) with a mass defect range from 26.5 to 126.5 mDa and mass range from 395 to 495 Da. The substructure filter was based on the location of baicalein ($C_{15}H_{19}O_5$) with a mass defect range from −5.0 to 95.0 mDa and mass range from 219 to 319 Da. Three types of conjugate filters, including glucuronide and sulfate were also applied herein, including baicalin + glucuronide with a mass defect range from 58.6 to 158.6 mDa and mass range from 571 to 671 Da, baicalin + sulfate with a mass defect range from −17.0 to 83.0 mDa and mass range from 475 to 575 Da, and baicalein + sulfate with a mass defect range from −50.0 to 50.0 mDa and mass range from 299 to 399 Da. Overall, the post-acquisition data processing technology was successfully applied to investigate the major-to-trace metabolites of baicalin from the complex background noise and endogenous components.

Table 1
Summary of baicalin metabolites in rat plasma, urine, and six kinds of tissues.

Peak	t_R min	Theoretical Mass m/z	Experimental Mass m/z	Error (ppm)	Formula $[M-H]^-$	MS/MS fragments	Identification	Clog P	Plasma	Urine	Heart	Liver	Spleen	Lung	Kidney	Brain
M1	7.18	461.0714	461.0719	0.45	$C_{21}H_{17}O_{12}$	MS^2 [461]: 285(100) MS^3 [285]: 267(100), 213(62), 239(57)	5,7,8-Trihydroxyflavone-6-*O*-glucuronide	−0.118	+	–	–	–	–	–	–	–
M2	7.65	461.0714	461.0724	1.00	$C_{21}H_{17}O_{12}$	MS^2 [461]: 267(100), 443(46), 285(16), 175(7) MS^3 [267]: 239(100), 143(1)	5,6,8-Trihydroxyflavone-7-*O*-glucuronide	−0.118	+	+	–	–	–	–	–	–
M3	8.66	461.0714	461.0725	1.03	$C_{21}H_{17}O_{12}$	MS^2 [461]: 443(100), 267(24), 285(15), 193(2) MS^3 [443]: 267(100),	6,7,8-Trihydroxyflavone-5-*O*-glucuronide	−0.802	+	+	–	–	–	–	–	–
M4	8.90	621.1086	621.1093	0.68	$C_{27}H_{25}O_{17}$	MS^2 [621]: 445(100)	5-Hydroxyflavone-7-*O*-glucuronide-8-*O*-glucuronide	−1.348	+	+	–	–	–	–	–	–
M5	9.41	475.0870	475.0876	0.45	$C_{22}H_{19}O_{12}$	MS^2 [475]: 299(100), 175(14) MS^3 [299]: 284(100) MS^4 [284]: 227(100), 228(85), 256(81)	5,8-Dihydroxy-6-methoxyflavone-7-*O*-glucuronide	0.127	+	+	–	–	–	–	–	–
M6[a]	9.67	461.0714	461.0722	0.79	$C_{21}H_{17}O_{12}$	MS^2 [461]: 285(100), 443(11)	5,6,4′-Trihydroxyflavone-7-*O*-glucuronide	0.145	+	–	–	–	–	–	–	–
M7	9.87	349.0012	349.0011	−0.10	$C_{15}H_9O_8S$	MS^2 [349]: 269(100) MS^3 [269]: 251(100), 241(54), 223(48), 197(35)	6,7-Dihydroxy-5-*O*-sulfate-flavone	0.605	–	+	–	–	–	–	–	–
M8[b]	10.03	607.1293	607.1301	0.77	$C_{27}H_{27}O_{16}$	MS^2 [607]: 431(100) MS^3 [431]: 269(100) MS^4 [269]: 251(100), 241(56), 223(40), 197(22)	5-Hydroxyflavone-6-*O*-glucoside-7-*O*-glucuronide	−1.119	+	–	+	+	+	+	+	+
M9	10.17	621.1086	621.1089	0.32	$C_{27}H_{25}O_{17}$	MS^2 [621]: 445(100) MS^3 [445]: 269(100)	5-Hydroxyflavone-6-*O*-glucopyranuronoside-7-*O*-glucopyranuronoside	−1.598	+	+	+	–	–	+	+	+
M10	10.64	475.0870	475.0877	0.58	$C_{22}H_{19}O_{12}$	MS^2 [475]: 299(100), 284(13) MS^3 [299]: 284(100)	5,8-Dihydroxy-7-methoxyflavone-6-*O*-glucuronide	0.127	+	+	–	+	–	–	+	–

M11	10.67	525.0333	525.0335	0.16	$C_{21}H_{17}O_{14}S$	MS^2 [525]: 445(100), 349(85), 255(32), 269(22) MS^3 [445]: 269(100)	5-Hydroxy-6-*O*-sulfate-flavone-7-*O*-glucuronide	−1.119	–	+	–	–	–	–	–	–
M12[b]	10.85	621.1086	621.1102	1.60	$C_{27}H_{25}O_{17}$	MS^2 [621]: 445(100)	8-Hydroxyflavone-5-*O*-glucuronide-7-*O*-glucuronide	−2.147	+	+	–	–	–	–	–	–
M13	10.94	475.0870	475.0879	0.81	$C_{22}H_{19}O_{12}$	MS^2 [475]: 299(100), 284(6), 175(6) MS^3 [299]: 284(100)	6,7-Dihydroxy-8-methoxyflavone-5-*O*-glucuronide	−0.352	+	+	–	+	–	–	+	–
M14	11.26	525.0333	525.0344	1.07	$C_{21}H_{17}O_{14}S$	MS^2 [525]: 445(100), 255(32), 349(21) MS^3 [445]: 269(100)	5-Hydroxy-7-*O*-sulfate-flavone-6-*O*-glucuronide	−1.449	–	+	–	–	–	–	–	–
M15	11.42	621.1086	621.1099	1.23	$C_{27}H_{25}O_{17}$	MS^2 [621]: 445(100)	6-Hydroxyflavone-5-*O*-glucuronide-7-*O*-glucuronide	−2.398	+	+	–	–	–	–	–	–
M16	11.60	525.0333	525.0338	0.46	$C_{21}H_{17}O_{14}S$	MS^2 [525]: 349(100), 269(25), 255(25), 445(11) MS^3 [349]: 269(100)	6-Hydroxy-7-*O*-sulfate-flavone-5-*O*-glucuronide	−2.349	–	+	–	–	–	–	–	–
M17[a]	12.26	431.0973	431.0984	1.12	$C_{21}H_{19}O_{10}$	MS^2 [431]: 269(100) MS^3 [269]: 251(100), 241(58), 223(43), 169(25), 197(24)	5,6-Dihydroxyflavone 7-*O*-glucoside	3.081	+	+	–	+	+	–	+	–
M18	12.57	459.0922	459.0931	0.89	$C_{22}H_{19}O_{11}$	MS^2 [459]: 283(100), 268(49)	6-Hydroxy-5-methoxyflavone-7-*O*-glucuronide	0.163	+	–	–	–	–	–	–	–
M19[b]	13.06	459.0922	459.0934	1.25	$C_{22}H_{19}O_{11}$	MS^2 [459]: 283(100), 175(16) MS^3 [283]: 268(100)	5-Hydroxy-6-methoxyflavone-7-*O*-glucuronide	0.963	+	+	+	+	+	+	+	+
M20	13.37	475.0870	475.0884	1.34	$C_{22}H_{19}O_{12}$	MS^2 [475]: 299(100), 284(17) MS^3 [299]: 284(100)	5,6-Dihydroxy-8-methoxyflavone-7-*O*-glucuronide	0.377	+	+	–	–	–	–	–	–
M21	13.47	459.0922	459.0932	1.04	$C_{22}H_{19}O_{11}$	MS^2 [459]: 283(100), 269(46), 175(15), 153(1)	5-Hydroxy-7-methoxyflavone-6-*O*-glucuronide	0.963	+	+	–	–	–	–	–	–
M22	13.66	475.0881	475.0883	1.15	$C_{22}H_{19}O_{12}$	MS^2 [475]: 299(100) MS^3 [299]: 284(100) MS^4 [284]: 255(100), 228(67), 256(62)	6,8-Dihydroxy-5-methoxyflavone-7-*O*-glucuronide	−0.672	+	+	–	–	–	–	–	–

Table 1 (*Continued*)

Peak	t_R min	Theoretical Mass *m/z*	Experimental Mass *m/z*	Error (ppm)	Formula $[M-H]^-$	MS/MS fragments	Identification	Clog *P*	Plasma	Urine	Heart	Liver	Spleen	Lung	Kidney	Brain
M23[a]	13.76	459.0922	459.0931	0.89	$C_{22}H_{19}O_{11}$	MS^2 [459]: 283(100), 175(25), 153(2) MS^3 [283]: 239(100), 240(76), 196(53)	5-Hydroxy-8-methoxyflavone-7-*O*-glucuronide	1.213	+	–	–	–	–	–	–	–
M24[b]	14.69	445.0765	445.0777	1.13	$C_{21}H_{17}O_{11}$	MS^2 [445]: 269(100) MS^3 [269]: 241(100), 251(94), 223(69), 207(45)	6,7-Dihydroxyflavone-5-*O*-glucuronide	–0.061	+	–	–	–	–	–	–	+
M25[a,b]	13.89	445.0765	445.0774	0.85	$C_{21}H_{17}O_{11}$	MS^2 [445]: 269(100) MS^3 [269]: 251(100), 241(64), 223(49), 197(30)	5,6-Dihydroxyflavone-7-*O*-glucuronide	0.769	+	+	+	+	+	+	+	–
M26	15.04	349.0012	349.0013	0.08	$C_{15}H_9O_8S$	MS^2 [349]: 269(100) MS^3 [269]: 251(100), 223(47), 169(26)	5,7-Dihydroxy-6-*O*-sulfate-flavone	1.435	–	+	–	–	–	–	–	–
M27	15.13	445.0765	445.0777	1.13	$C_{21}H_{17}O_{11}$	MS^2 [445]: 269(100) MS^3 [269]: 251(100), 241(64), 223(36), 195(25)	5,7-Dihydroxyflavone-6-*O*-glucuronide	0.519	+	–	–	–	–	–	–	–
M28	15.52	475.0870	475.0883	1.15	$C_{22}H_{19}O_{12}$	MS^2 [475]: 299(100), 284(15) MS^3 [299]: 284(100)	5,6-Dihydroxy-4′-methoxyflavone-7-*O*-glucuronide	0.690	+	–	–	–	–	–	–	–
M29[b]	15.80	349.0012	349.0017	0.48	$C_{15}H_9O_8S$	MS^2 [349]: 269(100) MS^3 [269]: 251(100), 241(57), 223(48), 197(35)	5,6-Dihydroxy-7-*O*-sulfate-flavone	1.435	–	+	–	+	–	–	+	–
M30[b]	15.96	283.0601	283.0609	0.75	$C_{16}H_{11}O_5$	MS^2 [283]: 268(100) MS^3 [283]: 239(100), 240(87), 183(54)	5,7-Dihydroxy-6-methoxyflavone	3.081	+	+	+	+	+	+	+	+
M31[b]	16.88	283.0601	283.0609	0.75	$C_{16}H_{11}O_5$	MS^2 [283]: 268(100) MS^3 [283]: 239(100), 240(95), 184(48)	5,6-Dihydroxy-7-methoxyflavone	3.331	+	+	–	–	–	–	–	–
M32[a,b]	18.68	269.0444	269.0452	0.69	$C_{15}H_9O_5$	MS^2 [269]: 251(100), 241(61), 223(49), 169(26), 197(25)	5,6,7-Trihydroxyflavone	3.002	+	–	–	+	–	–	+	–
									26	23	5	9	5	5	10	5

+: Being detected in the sample.

–: Not being detected in the sample.

[a] Metabolites identified by comparison with reference standards.

[b] Metabolites reported in the bibliography data.

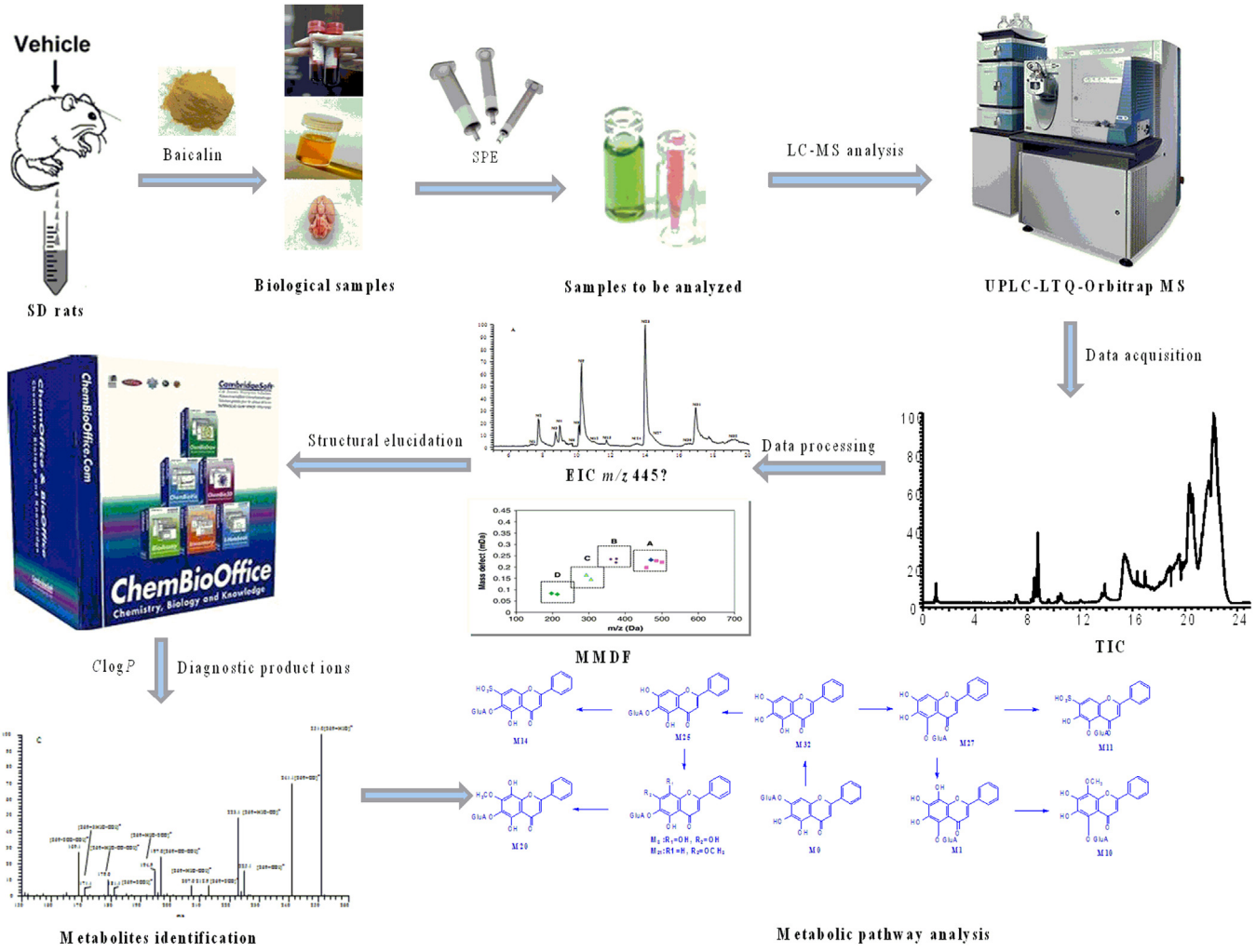

Fig. 2. Summary diagram of presently developed analytical strategy and methodology for detection and identification of baicalin metabolites.

3.4. Fragmentation behaviors of the reference compounds in negative ion mode

To facilitate the structural identification of the metabolite, Mass Frontier 7.0 software and manual elucidation were used to propose the fragmentation behaviors of five reference compounds with similar structure representing the major structural types of the baicalin metabolites. Taking baicalin for example (shown in Fig. 3), it exhibited $[M-H]^-$ ion at *m/z* 445.0774 (error 0.85 ppm, $C_{21}H_{17}O_{11}$) in the ESI-MS spectrum. In the ESI-MS^2 spectrum, it yielded $[M-H-176]^-$ ion at *m/z* 269 by neutral loss of a glucuronic acid residue. The neutral loss can be used for the identification of *O*-glucuronides. In the ESI-MS^3 spectra, the base peak at *m/z* 241 and the predominant ion at *m/z* 251 were generated by the loss of CO from the 4-position and H_2O from the 5,6,7-tri-OH group, respectively. Meanwhile, an ion at *m/z* 223 was yielded by the subsequent loss of H_2O from the ion at *m/z* 241. The ion at *m/z* 251 produced the product ion at *m/z* 207 owing to the neutral loss of CO_2 from the 1-O and 4-CO positions. Moreover, the minor ions including $[269-CO_2]^-$ ion at *m/z* 225, $[269-2CO]^-$ ion at *m/z* 213, $[269-H_2O-CO_2]^-$ ion at *m/z* 207, $[269-CO-CO_2]^-$ ion at *m/z* 197, $[269-CO-CO_2]^-$ ion at *m/z* 197, $[269-H_2O-2CO]^-$ ion at *m/z* 195, $[269-H_2O-CO-CO_2]^-$ ion at *m/z* 179, $[269-3H_2O-CO_2]^-$ ion at *m/z* 171, and $[269-2CO-CO_2]^-$ ion at *m/z* 169 were also observed in its ESI-MS^3 spectrum. These diagnostic fragmentation pathways mentioned above could be adopted to rapidly determine the structural skeletons and substitution patterns of metabolites in the complex matrices.

3.5. Identification of the metabolites of baicalin in rats

Thermo Xcalibur 2.1 and Metworks software were used to analyze the data of all dosed samples and their corresponding blank samples. The main criteria to search for metabolites were strong induction in test samples and the absence in blank control ones. Matrices derived signals made finding metabolites extremely challenging, which meant interference and ionization suppression induced by high abundance endogenous compounds could strongly prevent the detection of metabolites in total ion chromatograms (TIC). However, with the high selectivity of EIC-MS and MMDF methods, most of the baicalin metabolites showed high specificity. According to the search results, 32 baicalin metabolites (**M1**–**M32**) were detected (shown in Fig. 4). Among them, **M6**, **M17**, **M23**, **M25**, and **M32** were unambiguously identified by comparing their retention times and mass spectra with those of authentic compounds. Other metabolites were tentatively characterized on the basis of mass fragmentation pathways of the flavonoids from *S. baicalensis* [17].

Meanwhile, there were usually a number of metabolites isomers in biological matrices, which made it a difficult job to discriminate the exact conjugation site by LC–MS analysis. Therefore, the

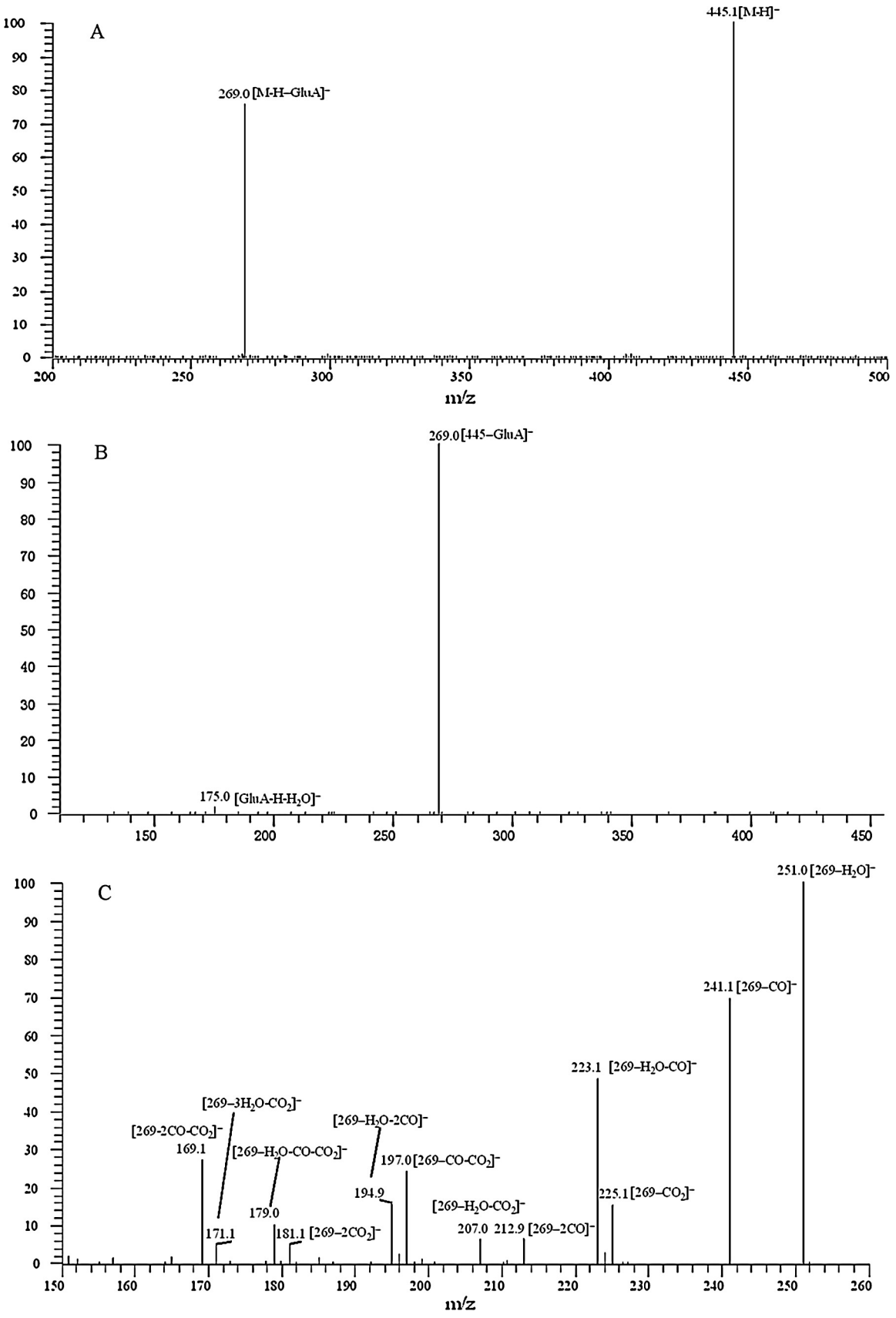

Fig. 3. ESI-MS^n spectra of baicalin: (A) MS spectrum; (B) MS^2 spectrum (precursor-ion was *m*/*z* 445); (C) MS^3 spectrum (precursor-ion was *m*/*z* 269).

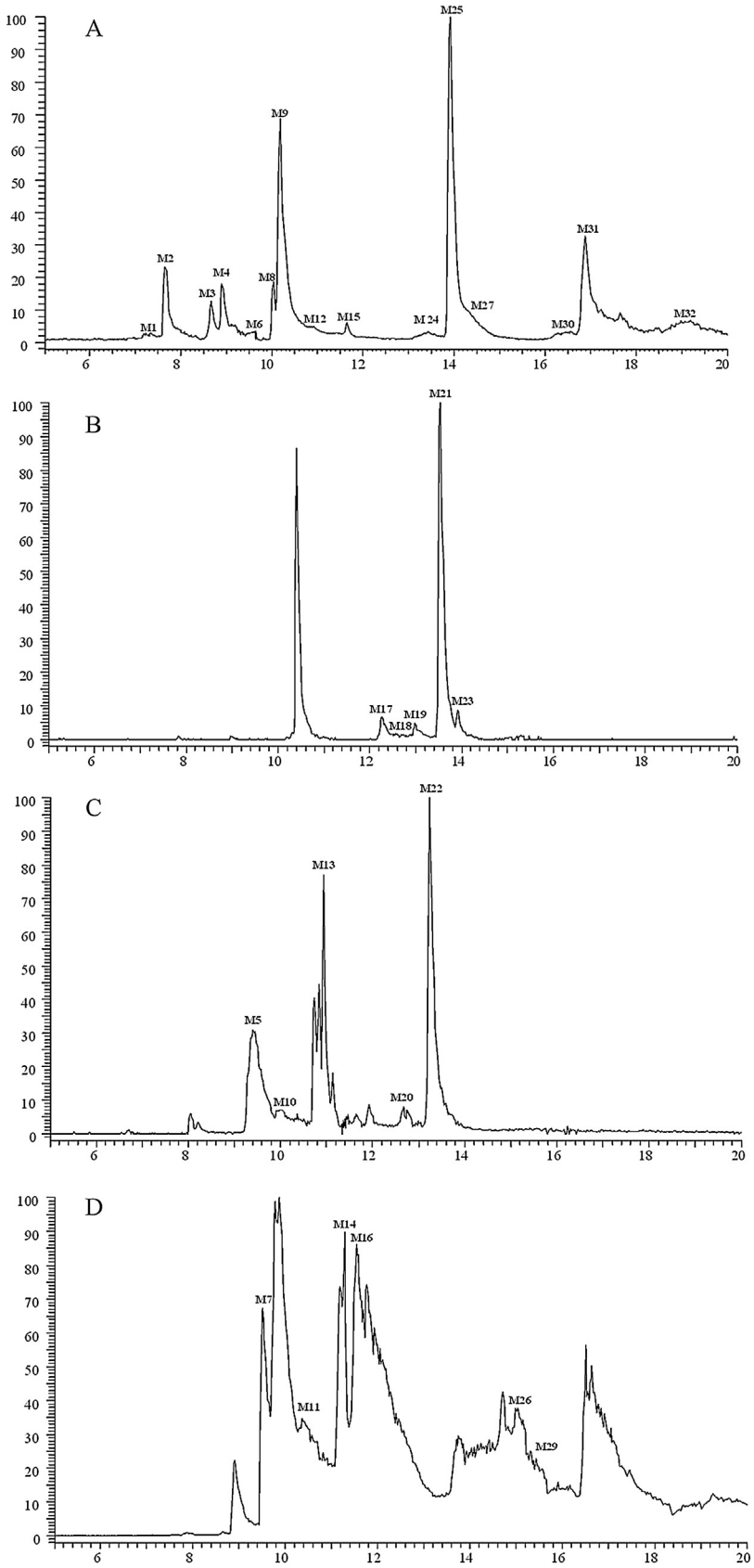

Fig. 4. The sum of high-resolution EIC in 5 ppm for the multiple metabolites in rat plasma and urine (A) *m*/*z* 461.0714, 621.1086, 607.1293, 445.0765, 283.0601, 269.0444; (B) *m*/*z* 431.0973, 459.0922; (C) *m*/*z* 475.0870, 525.0333, 349.0012; (D) *m*/*z* 349.0012, 525.0333.

parameter of *C*log *P* was adopted to determine the conjugation site. *C*log *P* is the calculated value of log *P* (*n*-octanol/water partition coefficient), which is predicated by the software ChemBioDraw Version 11.0 (Cambridge-Soft, Cambridge, MA, USA) based on theoretical calculations. It is useful to evaluate the hydrophobicity of a certain compound. Generally, the compound with larger *C*log *P* value would yield a larger retention time on reverse-phase HPLC [18,19,11].

3.5.1. Identification of **M1–3**, **M6**, **M24–25**, **M27**, and **M32**

M25 and **M32** possessed similar retention time, $[M-H]^-$ion, and MS/MS spectra with baicalin (5,6-dihydroxyflavone-7-*O*-glucuronide) and baicalein (5,6,7-trihydroxyflavone), respectively, which indicated that the prototype drug might be absorbed into the blood through two possible metabolic pathways. In the first pathway, baicalin is absorbed into the blood and metabolized to baicalein by a glucuronate enzyme. In the second pathway, baicalin is first biotransformed into baicalein in the gastrointestinal (GI) tract and baicalein is then absorbed into the blood [20]. It had been reported that baicalein with *m*/*z* of 269 $[M-H]^-$could easily be found in rat plasma after oral administration. Therefore, it could be concluded easily that baicalin is metabolized into baicalein in the GI tract, and baicalein is reconjugated with glucuronate and then excreted into the urine. Moreover, the occurrences of **M24** and **M27** in the plasma also validated the conclusion deduced above. Since it is much easier to observe glucuronide conjugation occurring to hydroxy groups on 5, 6, or 7 positions of baicalein, they were respectively identified as 6,7-dihydroxyflavone-5-*O*-glucuronide and 5,7-dihydroxyflavone-6-*O*-glucuronide [5] by referring to their *C*log *P* values.

M1, **M2**, **M3**, and **M6** were respectively eluted at 7.18, 7.65, 8.66, and 9.67 min and produced their deprotonated molecular ions at *m*/*z* 461.07 ($C_{21}H_{17}O_{12}$). It could be deduced that they was hydroxylated product of **M24**, **M25**, and **M27**. **M6** was unambiguously identified as scutellarin (5,6,4′-trihydroxyflavone-7-*O*-glucuronide) by comparison with the reference standard. By analyzing their product ions in the ESI-MS/MS spectra, **M1**, **M2**, and **M3** were presumed to be 5,7,8-trihydroxyflavone-6-*O*-glucuronide, 5,6,8-trihydroxyflavone-7-*O*-glucuronide, and 6,7,8-trihydroxyflavone-5-*O*-glucuronide, respectively.

3.5.2. Identification of **M11**, **M14**, and **M16**

M11, **M14**, and **M16**, whose retention times were 10.67, 11.26 and 11.60 min, respectively, generated the same $[M-H]^-$ ions at *m*/*z* 525.03. In their MS^2 spectra, there was abundant product ion at *m*/*z* 445 by the neutral loss of 80 Da. Other diagnostic fragment ions, *viz*., $[M-H-GluA]^-$ at *m*/*z* 349 and $[M-H-GluA-SO_3]^-$ at *m*/*z* 269 were all observed, indicating that both of the metabolites were dihydroxyflavone-*O*-glucuronide sulfates. Considering that there have been three characterized baicalin metabolites with the same mass weight of 445 Da, **M11**, **M14**, and **M16** were plausibly deduced as 5-hydroxy-6-*O*-sulfate-flavone-7-*O*-glucuronide, 5-hydroxy-7-*O*-sulfate-flavone-6-*O*-glucuronide, and 6-hydroxy-7-*O*-sulfate-flavone-5-*O*-glucuronide, respectively [21].

3.5.3. Identification of **M7**, **M26**, and **M29**

Metabolites **M7**, **M26**, and **M29** were eluted at 9.87, 15.04 and 15.80 min, respectively. They all yielded the deprotonated molecular ion at *m*/*z* 349.00 with molecular formula $C_{15}H_9O_8S$. Their ESI-MS^2 base peak ions at *m*/*z* 269 were generated by neutral loss of 80 Da, suggesting they were trihydroxyflavone sulfates. Their aglycones produced the same product ions at *m*/*z* 251, *m*/*z* 241, and *m*/*z* 223, which were consistent with those of **M32**. Therefore, they were identified as 6,7-dihydroxy-5-*O*-sulfate-flavone, 5,7-dihydroxy-6-*O*-sulfate-flavone, and 5,6-dihydroxy-7-*O*-sulfate-flavone, respectively [22].

3.5.4. Identification of **M30** and **M31**

Metabolite **M30** and **M31** eluted at 15.96 and 16.88 min, generated the deprotonated molecular ion at *m*/*z* 283.06 ($C_{16}H_{11}O_5$). In their MS^2 spectra, $[M-H-CH_3^{\bullet}]^-$ at *m*/*z* 268 was all observed, suggesting that it could be attributed to dihydroxy-monomethoxyflavone, and proposed as methylation metabolite of baicalein. Therefore, they were tentatively identified as 5,7-dihydroxy-6-methoxyflavone and 5,6-dihydroxy-7-methoxyflavone, respectively [8].

3.5.5. Identification of **M5**, **M10**, **M13**, **M18–23**, and **M28**

Metabolites **M18**, **M19**, **M21**, and **M23** were eluted at 12.57, 13.06, 13.47, and 13.76 min, respectively. All of them yielded the same $[M-H]^-$ ions at *m*/*z* 459.09. In the MS^2 spectra, there was abundant product ion at *m*/*z* 283 by the neutral loss of 176 Da, indicating that they were glucuronide conjugates. In their ESI-MS/MS, the $[M-H-GluA-CH_3^{\bullet}]^-$ ion at *m*/*z* 268 generated by neutral loss of $CH_3^{\bullet}$ from the ion at *m*/*z* 283, indicating that they could be tentatively confirmed as baicalein methylates. **M23** was unambiguously identified as wogonoside (5-hydroxyl-8-methoxyflavone-7-*O*-glucuronide) by comparison with the reference standard. By investigating the literature data and their *C*log *P* values, the other three baicalin metabolites were presumed to be 6-hydroxy-5-methoxyflavone-7-*O*-glucuronide, 5-hydroxy-6-methoxyflavone-7-*O*-glucuronide, and 5-hydroxy-7-methoxyflavone-6-*O*-glucuronide, respectively [23].

M5, **M10**, **M13**, **M20**, **M22**, and **M28** were respectively eluted at 9.41, 10.94, 13.37, 13.66, and 15.51 min with the same $[M-H]^-$ ions at *m*/*z* 475.09 ($C_{22}H_{19}O_{12}$), which were 16 Da more than that of **M18**, **M19**, and **M21** (*m*/*z* 459.09), or 14 Da more than that of **M2**, **M3**, and **M6** (*m*/*z* 461.07). It could be deduced that hydroxylation occurred to **M18**, **M19** and **M21** or methylation occurred to **M2**, **M3**, and **M6**. Therefore, they were tentatively confirmed as 5,8-dihydroxy-6-methoxyflavone-7-*O*-glucuronide, 5,8-dihydroxy-7-methoxyflavone-6-*O*-glucuronide, 6,7-dihydroxy-8-methoxyflavone-5-*O*-glucuronide, 5,6-dihydroxy-8-methoxyflavone-7-*O*-glucuronide, 5,6-dihydroxy-4′-methoxyflavone-7-*O*-glucuronide, and 6,8-dihydroxy-5-methoxyflavone-7-*O*-glucuronide, respectively.

3.5.6. Identification of **M4**, **M9**, **M12**, and **M15**

All the metabolites **M4**, **M9**, **M12**, and **M15** produced the same $[M-H]^-$ ions at *m*/*z* 621.10 ($C_{27}H_{25}O_{17}$) with 176 Da more than that of trihydroxyflavone, suggesting that they were glucuronide metabolites of baicalin. The occurrences of fragment ions including $[M-H-GluA]^-$at *m*/*z* 445 and $[M-H-2GluA]^-$at *m*/*z* 269, have also validated the conclusion deduced above. By examining the reported flavonoids, their aglycones were tentatively confirmed as 5,6,7-trihydroxyflavone and 5,7,8-trihydroxyflavone. Analyzing the *C*log *P* values of their potential glycosides, they were tentatively assigned as 5-hydroxyflavone-7-*O*-glucuronide-8-*O*-glucuronide, 5-hydroxyflavone-6-*O*-glucopyranuronoside-7-*O*-glucopyranuronoside, 8-hydroxyflavone-5-*O*-glucuronide-7-*O*-glucuronide, and 6-hydroxyflavone-5-*O*-glucuronide-7-*O*-glucuronide, respectively [23].

3.5.7. Identification of **M8** and **M17**

M17 was eluted at 12.26 min and produced its $[M-H]^-$ ion at *m*/*z* 431.0984 (error 1.12 ppm, $C_{21}H_{19}O_{10}$). It could be unambiguously identified as Oroxin A (5,6-dihydroxyflavone-7-*O*-glucoside) by comparison with the reference standard, and it could be assigned as glucoside conjugates product of baicalein. **M8** yielded its $[M-H]^-$ ion at *m*/*z* 607.1301 (error 0.77 ppm, $C_{27}H_{27}O_{16}$),

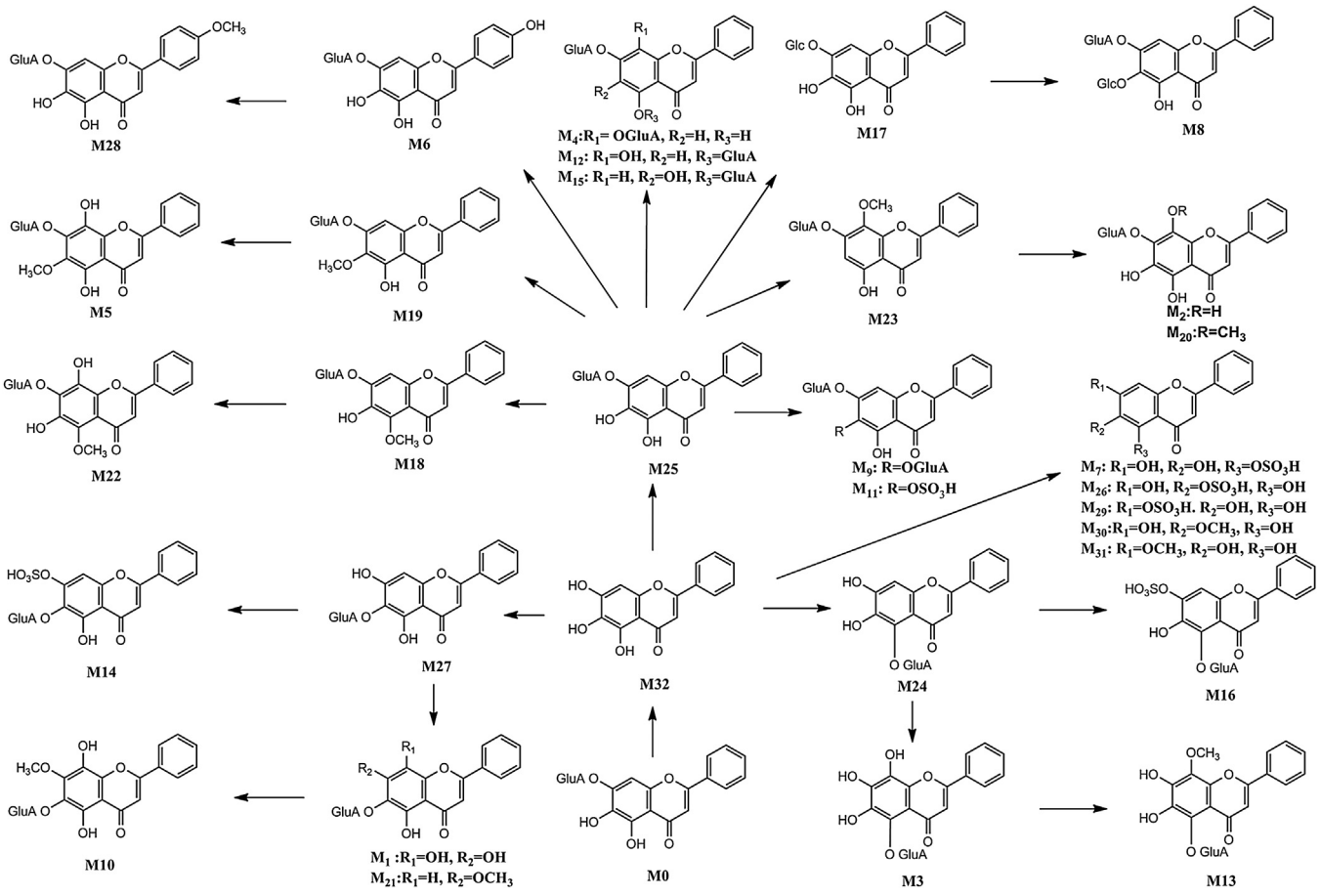

Fig. 5. The proposed baicalin metabolic pathways in the plasma and urine of SD rats.

whose molecular weight is 176 Da more than that of **M17**. By investigating the literature data [23], **M8** was presumed to be 5,6,7-trihydroxyflavone-6-*O*-glucoside-7-*O*-glucuronide.

3.6. Proposed metabolic pathways of baicalin

In this study, a total of 32 metabolites with different structures were observed and identified in SD rats after the oral administration of baicalin. Among them, 26 metabolites were detected in the rat plasma and 23 metabolites were identified in the rat urine. The proposed major metabolic pathway of baicalin in the rat plasma and urine is demonstrated in Fig. 5. Our results indicated that the hydroxyl groups on A ring and 8-, 4′ positions of baicalin were the major metabolic sites. Furthermore, baicalin mainly underwent methylation, hydrolysis, hydroxylation, methoxylation, glucuronide conjugation, sulfate conjugation, and their composite metabolic reactions. Although many types of conjugate filters, including glucuronide, sulfate, glutathione (GSH), and N-acetylcysteine (NAC), were established preliminarily, only the metabolic conjugation with sulfate and glucuronide were detected.

3.7. Distribution of the baicalin metabolites in rat tissues

The distribution of 32 metabolites in rat tissues was studied for the first time (shown in Table 1). The results demonstrated that five metabolites were detected in heart, including **M8**, **M9**, **M19**, **M25**, and **M30**. In the liver, nine metabolites (**M8**, **M10**, **M13**, **M17**, **M19**, **M25**, **M29**, **M30**, and **M32**) were detected. In the spleen, five metabolites (**M8**, **M17**, **M19**, **M25**, and **M30**) were found. In the lung, five metabolites (**M8**, **M9**, **M19**, **M25**, and **M30**) were found, and five metabolites (**M8**, **M9**, **M19**, **M24**, and **M30**) were observed in the brain of rats. Ten metabolites including **M8**, **M9**, **M10**, **M13**, **M17**, **M19**, **M25**, **M29**, **M30**, and **M32**, were found in the kidney of rats. According to our results, it could be deduced that the liver is also an important organ for the distribution of metabolites of baicalin except for the kidney. In the brain, **M8**, **M9**, **M19**, **M24**, and **M30** were detected, which hinted that they might be easier to pass through the blood brain barrier, and responsible for the pharmacological actions of baicalin on the brain. In addition, **M8**, **M9**, **M17**, **M19**, **M25**, and **M30** were distributed more widely than the other metabolites. **M8**, **M19**, and **M30** existed in all of the organs we examined; **M17** existed in the liver, spleen, and kidney; **M25** existed in the heart, liver, spleen, lung, and kidney. Hence, these six metabolites might play an important role in exerting pharmacological effects of baicalin *in vivo*, and their pharmacological actions deserve further investigation.

4. Conclusions

It is well known that the structural elucidation of metabolites is one of the most challenging tasks in drug metabolism studies. The established UPLC/ESI-LTQ-Orbitrap MS^n method was applied to analyze the *in vivo* metabolism of baicalin in rats. By on-line LC–MS^n data acquisition and off-line data processing methods of the software Xcalibur 2.1, a total of 32 metabolites were identified in the rat plasma and urine. Among them, 5 metabolites were unambiguously confirmed, while the others were tentatively identified. Meanwhile, 5 metabolites could be found in rat heart, 9 in liver, 5 in spleen, 5 in lung, 10 in kidney, and 5 in brain. The results demonstrated that the rat liver and kidney are the most important

organs for the distribution of baicalin metabolites, and **M8**, **M9**, **M17**, **M19**, **M25**, and **M30** might play an important role in exerting pharmacological effects of baicalin *in vivo*, which is also important to understand its pharmacological effects.

Different from the previous researches, we paid much more attention to major-to-trace metabolites of baicalin. The corresponding reactions *in vivo* such as methylation, hydrolysis, hydroxylation, methoxylation, glucuronide conjugation, sulfate conjugation, and their composite reactions, were all discovered in the study. The main advantage of LTQ-Orbitrap was that it could provide multi-stage MS^n mass spectra using data-dependent analysis and a higher mass resolution and mass accuracy than many other mass spectrometers. The study also provided a practical strategy for rapidly assaying major-to-trace metabolites with the aid of EIC and MMDF analysis. Besides, the results could provide comprehensive insights and guidance for elucidation of side effect mechanism and safety monitoring as well as for rational formulation design in drug delivery system. The newly discovered baicalin metabolites significantly expanded our understanding on its pharmacological effects, and could be targets for future studies on the important chemical constituent from herbal medicines.

Acknowledgements

The authors greatly appreciate the financial support from the National Foundation of Natural Sciences of China (81303206) and China Postdoctoral Science Foundation (no. 2013M530563).

References

[1] G.H. Can, E. Sofic, R.L. Prior, Antioxidant and prooxidant behavior of flavonoids: structure-activity relationships, Free Radic. Biol. Med. 22 (1997) 749.
[2] C.A. Williams, J.B. Harborne, H. Geiger, J. Robin, S. Hoult, The flavonoids of Tanacetum parthenium and T. vulgare and their anti-inflammatory properties, Phytochemistry 51 (1999) 417.
[3] A. Mantas, E. Detetey, F.H. Ferretti, M.R. Estrada, I.G. Csizmadia, Structural analysis of flavonoids with anti-HIV activity, J. Mol. Struct. (Theochem.) 504 (2000) 171.
[4] M.Y. Lai, S.L. Hsiu, S.Y. Tsai, Y.C. Hou, P.D. Lee Chao, Comparison of metabolic pharmacokinetics of baicalin and baicalein in rats, J. Pharm. Pharmacol. 55 (2003) 205.
[5] M. Holčapek, L. Kolárová, M. Nobilis, High-performance liquid chromatography–tandem mass spectrometry in the identification and determination of phase I and phase II drug metabolites, Anal. Bioanal. Chem. 391 (2008) 59.
[6] K. Levsen, H.M. Schiebel, B. Behnke, R. Dötzer, W. Dreher, M. Elend, H. Thiele, Structure elucidation of phase II metabolites by tandem mass spectrometry: an overview, J. Chromatogr. A 1067 (2005) 55.
[7] N.P. Feng, B. Di, W.Y. Liu, Comparison of the metabolism of baicalin in rats orally administered with Radix scutellariae extract and Shuang-Huang-Lian extract, Chem. Pharm. Bull. 53 (2005) 978.
[8] Y. Wang, J.Y. Yang, X. Li, J.H. Wang, The metabolism of baicalin in rat and the biological activities of the metabolites, Evid. Based Complement. Altern. Med. 2012 (2012) 404529.
[9] F. Zuo, Z.M. Zhou, M.Z. Yan, M.L. Liu, Y.L. Xiong, Q. Zhang, H.Y. Song, W.H. Ye, Metabolism of constituents in Huangqin-Tang, a prescription in traditional Chinese medicine, by human intestinal flora, Biol. Pharm. Bull. 25 (2002) 558.
[10] F. Zuo, Z.M. Zhou, Q. Zhang, D. Mao, Y.L. Xiong, Y.L. Wang, M.Z. Yan, M.L. Liu, Pharmacokinetic study on the multi-constituents of Huangqin-Tang decoction in rats, Biol. Pharm. Bull. 26 (2003) 911.
[11] J. Liang, F. Xu, Y.Z. Zhang, S. Huang, X.Y. Zang, X. Zhao, L. Zhang, M.Y. Shang, D.H. Yang, X. Wang, S.Q. Cai, The profiling and identification of the absorbed constituents and metabolites of Paeoniae Radix Rubra decoction in rat plasma and urine by the HPLC–DAD–ESI-IT-TOF-MSn technique: A novel strategy for the systematic screening and identification of absorbed constituents and metabolites from traditional Chinese medicines, J. Pharm. Biomed. 83 (2013) 108.
[12] J.Y. Zhang, F. Wang, W. Cai, Q. Zhang, Y. Liu, Y. Li, R.R. Liu, G.S. Cao, Identification of metabolites of gardenin A in rats by combination of high-performance liquid chromatography and linear ion trap–Orbitrap mass spectrometer based on multiple data processing techniques, Biomed. Chromatogr. (2014) 3287, http://dx.doi.org/10.1002/bmc.
[13] T. Xie, Y. Liang, H.P. Hao, AJ, L. Xie, P. Gong, C. Dai, L.S. Liu, A. Kang, X. Zheng, G.J. Wang, Rapid identification of ophiopogonins and ophiopogonones in Ophiopogon japonicus extract with a practical technique of mass defect filtering based on high resolution mass spectrometry, J. Chromatogr. A 1227 (2012) 234.
[14] M.Y. Liu, S.H. Zhao, Z.Q. Wang, Y.F. Wang, T. Liu, S. Li, C.C. Wang, H.T. Wang, P.F. Tu, Identification of metabolites of deoxyschizandrin in rats by UPLC–Q-TOF-MS/MS based on multiple mass defect filter data acquisition and multiple data processing techniques, J. Chromatogr. B 949 (2014) 115.
[15] Y. Liang, W. Xiao, C. Dai, L. Xie, G.G. Ding, j. Wang, Z.Q. Meng, J. Zhang, A. Kang, T. Xie, Y.N. Liu, Y.Y. Zhou, W.J. Liu, L. Zhao, J. Xu, Structural identification of the metabolites for strictosamide in rats bile by an ion trap-TOF mass spectrometer and mass defect filter technique, J. Chromatogr. B 879 (2011) 1819.
[16] J.Y. Zhang, Q. Zhang, H.X. Zhang, Q. Ma, J.Q. Lu, Y.J. Qiao, Characterization of polymethoxylated flavonoids (PMFs) in the peels of 'Shatangju' mandarin (Citrus reticulata Blanco) by online high-performance liquid chromatography coupled to photodiode array detection and electrospray tandem mass spectrometry, J. Agric. Food Chem. 60 (2012) 9023.
[17] G.Z. Liu, J.Y. Ma, Y.Z. Chen, Q.Q. Tian, Y. Shen, X.S. Wang, B. Chen, S.Z. Yao, Investigation of flavonoid profile of Scutellaria bacalensis Georgi by high performance liquid chromatography with diode array detection and electrospray ion trap mass spectrometry, J. Chromatogr. A 1216 (2009) 4809.
[18] Y.Z. Zhang, F. Xu, J. Dong, J. Liang, Y. Hashi, M.Y. Shang, D.H. Yang, X. Wang, S.Q. Cai, Profiling and identification of the metabolites of calycosin in rat hepatic 9000× g supernatant incubation system and the metabolites of calycosin-7-O-β-d-glucoside in rat urine by HPLC–DAD–ESI–IT–TOF–MS n technique, J. Pharm. Biomed. 70 (2012) 425.
[19] M.Y. Liu, S.H. Zhao, Z.Q. Wang, Y.F. Wang, T. Liu, S. Li, C.C. Wang, H.T. Wang, P.F. Tu, Identification of metabolites of deoxyschizandrin in rats by UPLC–Q–TOF–MS/MS based on multiple mass defect filter data acquisition and multiple data processing techniques, J. Chromatogr. B 949–950 (2014) 115.
[20] Q.M. Che, X.L. Huang, Y.M. Li, K. Zhang, A. Teruaki, H. Masao, Studies on metabolites of baicalin in human urine, Chin. J. Chin. Mater. Med. 26 (2001) 768.
[21] K. Abe, O. Inoue, E. Yumioka, Biliary excretion of metabolites of baicalin and baicalein in rats, Chem. Pharm. Bull. 38 (1990) 20.
[22] M.Y. Lai, S.L. Hsiu, C.C. Chen, Y.C. Hou, P.D.L. Chao, Urinary pharmacokinetics of Baicalein, Wogonin and their glycosides after oral administration of Scutellariae Radix in humans, Biol. Pharm. Bull. 26 (2003) 79.
[23] B. Di, N.P. Feng, W.Y. Liu, Study on metabolism differences of baicalin in compound Shuanghuanglian and Huangqin extract in rats, Chin. Pharm. J. 2 (2005) 50.